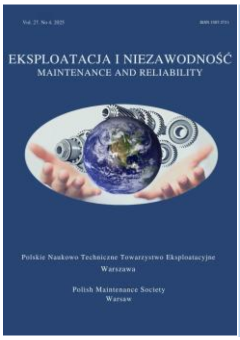

Eksploatacja i Niezawodnosc – Maintenance and Reliability
Volume 27 (2025), Issue 4
journal homepage: http://www.ein.org.pl

Article citation info:
Wang R, Wang J, Liu Y, Wang N, Detecting damages for wind turbine blades based on Chebyshev polynomial approximation and uniform load surface curvature, Eksploatacja i Niezawodnosc – Maintenance and Reliability 2025: 27(4) http://doi.org/10.17531/ein/204575

Detecting damages for wind turbine blades based on Chebyshev polynomial approximation and uniform load surface curvature

Indexed by: Web of Science Group

Ruohao Wang[a,c], Jianlong Wang[a,c], Yi Liu[a,b], Naige Wang[a,c*]

[a] College of Mechanical and Electrical Engineering, Wenzhou University, Wenzhou 325035, PR China
[b] School of Mechanical and Electrical Engineering, Guilin University of Electronic Technology, Guilin, P.R.China
[c] Key Laboratory of Equipment Monitoring and Intelligent Operation and Maintenance under Extreme Working Conditions in the Province, Zhejiang, PR China

Highlights

- An reliable and effective method for detecting WT blade damage method is proposed.
- It reduces the requirements for the number of measurement points and modal order.
- The process is applied to NREL 5MW WT blade and achieved high-order accuracy result.

This is an open access article under the CC BY license (https://creativecommons.org/licenses/by/4.0/)

Abstract

Wind turbine blades are among the most critical components of a wind turbine. Cracking is the most prevalent type of the WT blades damage, making it essential to develop methods for early detection and precise assessment of crack locations and severity. This paper proposes a novel method based on uniform load surface (ULS) curvature variation for determining the damage location in wind turbine blades. The Chebyshev polynomial is utilized instead of the central difference method to calculate ULS curvature. This method only needs the first-order natural frequency of the WT blade to detect the damage of the WT blade, and the numerical simulation results show that its calculation accuracy has low requirements on the number of measurement points. An experimental platform was established to collect modal data and a model updating technique was employed to adjust the simulation model parameters. Consequently, this method enhances the traditional modal curvature approach, offering a more comprehensive and reliable technique for structural health monitoring of wind turbine blades.

Keywords

finite element method; damage detection method; Chebyshev polynomial approximation; uniform load surface curvature; wind turbine blade

1. Introduction

As wind power generation has become an increasingly vital source of green renewable energy, wind turbine blades, as critical components of the system, are often exposed to harsh environments, making them susceptible to various forms of damage, including surface depressions, delamination, and cracking[1-3]. Studies have shown that blade failures caused by cracks are particularly challenging to detect, highly destructive, and costly to repair. Engineers and technicians employ multi-directional inspection techniques and regular maintenance strategies to address this issue. This study aims to develop an effective method for detecting structural damage in wind turbine blades.

Currently, traditional blade damage detection methods, such as infrared thermal imaging[4], ultrasound[5], and visual inspection[6], are limited by environmental temperature, material properties, equipment costs, and other factors. To enhance efficiency and accuracy while reducing costs and technical complexity, many researchers have introduced novel

(*) Corresponding author.
E-mail addresses: wangnaige@wzu.edu.cn
R. Wang (ORCID: 0009-0008-6066-1966) 317564953@qq.com, J. Wang (ORCID: 0000-0001-8068-6468) jlwang@wzu.edu.cn, Y. Liu(ORCID:0000-0003-4335-4135) liuyi_aa1@163.com, N.Wang (ORCID: 0000-0003-2003-2600) wangnaige@wzu.edu.cn,

approaches for wind turbine blade structural damage detection, including digital image processing[7], laser scanning[8], machine learning[9-12], and nanomaterial sensors[13]. However, the effectiveness and feasibility of these methods require further validation. Among these, damage diagnosis techniques based on the modal parameters of blade vibrations are also gaining increasing attention[2, 14-18].

The method of diagnosing structural damage based on modal parameters dates back to the 1970s and was initially applied to beams, plates, and other structures in civil engineering[19]. Structural damage alters the system's stiffness, mass, and damping properties, reflected in measurable or calculable modal parameters such as natural frequencies and mode shapes. However, relying on a single modal parameter is insufficient; for instance, two damages located in different areas may exhibit the same natural frequency. Consequently, researchers have conducted extensive further studies on this topic. Pai P.F et al. [20] furthered research using the boundary effect detection (BED) method, employing a scanning laser vibrometer to measure the operational deflection shapes (ODS) of the beam and identify small damage locations. Viola et al. [21] proposed a method to identify damage in Timoshenko beams using modal test data, investigating the impact of cracks on the stiffness and uniform mass matrices by introducing the concept of local flexibility. Rodríguez et al. [22] presented the baseline stiffness method (BSM), which involves extracting the vibration modes, natural frequencies, and transverse stiffness of the beam before and after damage. The method analyzes the location and severity of the damage using singular value decomposition. Through the persistent efforts of researchers, fundamental modal parameters such as natural frequency and mode have been developed into more sensitive, complex, and user-friendly modal parameters. These advancements facilitate the diagnosis of plate and beam structures that more accurately reflect real-world conditions. Wei et al. [23] proposed the concepts of the damage location factor (DLF) matrix and the damage severity correction factor (DSCF) matrix from the perspective of strain energy. Identifying damage in plate structures was achieved through three steps: sensitive mode selection, damage localization, and quantification in plate-type structures. Huang et al. [24] proposed a modal frequency strain energy assurance criterion (MFSEAC), along with a modal flexibility and enhanced moth-flame optimization damage diagnosis method, to identify damage in a simply supported steel beam and a three-story shear steel frame. This approach partially addresses low computational efficiency and the lack of a susceptible damage index. Wang [25] proposed a variability of modal strain energy residuals to detect damage in pile foundations of high-pile wharves. They established a quantitative relationship between modal strain energy residual variability and the degree of local damage. Jian-Xiong Gao [26] incorporated the effects of natural aging and fatigue loading to assess the residual strength of wind turbine blades. The results indicated that temperature significantly influenced the properties of glass fiber reinforced polymer.

As research progressed, engineers and technicians discovered that using singular value decomposition to reveal damaged information lacks robustness. They identified certain physical quantities more sensitive to damage and offer improved robustness. Kim [27] utilized the second derivative of the frequency response function as a damage index, identifying structural damage by measuring the dynamic behavior of the beam under varying levels of excitation force. Sung et al. [28] proposed a modal flexibility acquisition method for detecting damage in Bernoulli-Euler beams using normalized uniform load surface (NULS) curvature. This approach effectively identifies both single and multiple damage locations. Research indicates that NULS curvature is more sensitive and robust to damage compared to the singular value decomposition method. Wu [29] successfully applied uniform load surface (ULS) curvature to 2D flat structures, achieving more accurate results. Jiang et al. [30] employed a two-step method to detect damage in tablet structures, achieving favorable results. The curvature modal shape subtraction indicator was utilized in the first stage for damage localization. In the second stage, a database establishing the relationship between natural frequency and damage severity was developed, and damage severity was evaluated using particle swarm optimization (PSO). Ruoyang Bai et al. [31]employed Gramian Angular Field (GAF) and Squeeze and Excitation (SE) techniques to overcome the limitations associated with extended time series encoding and generalization, thereby enhancing the feature extraction capabilities for fault diagnosis in rotating machinery.

The method for diagnosing structural damage in blades based on modal parameters originates from damage detection techniques for plates and beams. Geometrically, wind turbine blades can be considered as curved beams with variable cross-sections, which presents significant challenges. Nonetheless, many researchers have successfully applied this method to wind turbine blades. Wang et al. [32] conducted a dynamic analysis of fan blades using the finite element method (FEM). They detected damage locations by examining the mode shape difference curvature (MSDC) of the blades. Cadoret et al. [33] approximated the time-invariant model of a time-periodic system, derived a damage sensitivity index based on adaptive modal parameters, and applied Gaussian residuals to accommodate changes in the time-periodic system. Jiang et al. [34] utilized the singular value decomposition method to extract singular information from the operational deflection shapes (ODS) of fan blades and established a natural frequency database. They employed the whale optimization algorithm (WOA) to find the natural frequency closest to the damage within the database, enabling the localization and evaluation of blade damage. Pacheco-Chérrez [35] utilized operational modal analysis (OMA) to analyze the vibrations of wind turbine blades. They extracted acceleration time series generated by random excitation of the blades, highlighting the characteristics of the damaged blade using the frequency domain decomposition (FDD) algorithm. Chuangyan Yang[36] proposed an algorithm combining Gated Recurrent Unit (GRU) and Stacked Sparse Autoencoder (SSAE), integrating dynamic latent variable analysis with deep learning, which was successfully applied to the identification of wind power blade icing faults.

It is well known that damage has a minimal impact on the lower-order natural frequencies and modes, while higher-order natural frequencies and modes are often difficult to excite. The detection of blade damage using mode shape difference curvature (MSDC) heavily relies on higher-order modal data. Similarly, the method of creating a database to optimize and assess damage also necessitates higher-order natural frequencies to enhance the accuracy of the results. Therefore, this study proposes a uniform load surface (ULS) curvature method based on Chebyshev polynomial approximation, allowing for accurate and clear representation of the position and severity of damage using first-order vibration mode data. The remainder of this article is organized as follows: The next section provides a brief overview of the process for calculating ULS curvature using Chebyshev polynomial approximation. In the third section, a numerical example is presented to assess blade damage using Chebyshev-ULS curvature, along with the experimental results. In the fourth section, the method is applied to a larger blade model, with added noise to assess the universality and robustness of the approach. The fifth section concludes the article. The flow chart of the proposed method is shown in Figure 1.

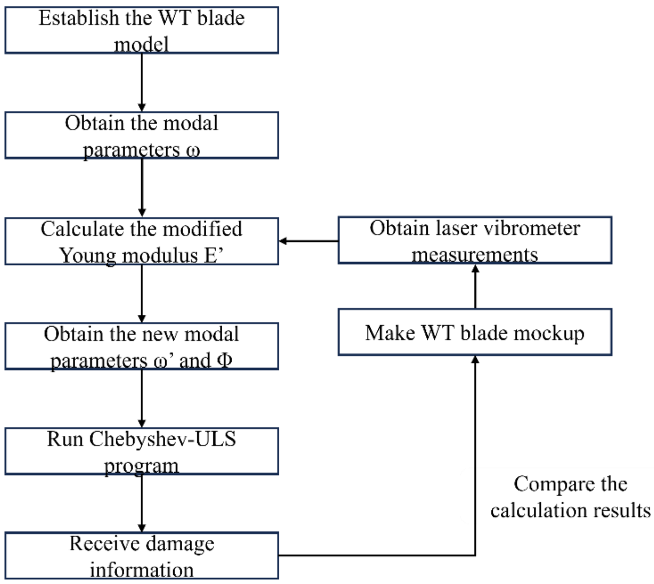

Figure 1. Flow chart of damage detection method.

2. Basic theory

2.1. Modal analysis

In general, the analysis can be reduced to a multi-degree-of-freedom system. By applying the Hamiltonian principle, the partial differential equation governing blade vibrations can be derived. The overall mass matrix, stiffness matrix, and damping matrix of the blade can then be obtained through discretization and assembly using the Galerkin method. In this context, the vibration equation of the blade can be simplified as follows:

$$\boldsymbol{M}\ddot{x} + \boldsymbol{C}\dot{x} + \boldsymbol{K}x = \boldsymbol{F} \tag{1}$$

where $\boldsymbol{M}$, $\boldsymbol{C}$, $\boldsymbol{K}$, and $\boldsymbol{F}$ represent the global mass matrix, damping matrix, global stiffness matrix, and external load vector of the blade, respectively. The matrices $\ddot{x}$, $\dot{x}$, and x denote the displacement, velocity, and acceleration matrices of the blade, respectively. The modal parameters obtained through modal analysis effectively represent the health status of the blade. Damage induces changes in the local element mass and stiffness matrices surrounding the damaged area, subsequently affecting the overall mass and stiffness matrices. Minor damage can be considered negligible for the total mass of the blade, meaning that external loads and damping do not influence the modal parameters. Essentially, the focus is on studying the free vibration system of the blade. Equation (1) can be simplified as follows:

$$\boldsymbol{M}\ddot{x} + \boldsymbol{K}x = \boldsymbol{0} \tag{2}$$

Any free vibration can be considered a form of harmonic motion. By substituting the displacement term of the blade back into the equation, the generalized characteristic equation of the blade can be derived:

$$(\boldsymbol{K} - \omega_i^2 \boldsymbol{M})\phi_i = 0 \tag{3}$$

In the above formula, ω represents the circular frequency of the blade, ϕ denotes the modal vector, i indicates the mode order of the blade, and $i = 1,2,\ldots,5$. The expressions for the blade's natural frequency, mass matrix, and stiffness matrix are provided below:

$$f_i = \frac{1}{2\pi}\sqrt{\frac{\boldsymbol{K}}{\boldsymbol{M}}} \tag{4}$$

Since the measured natural frequency of a real blade is influenced by its geometric dimensions, material properties, and environmental conditions, the natural frequency calculated from the finite element model represents an ideal state. This discrepancy can result in a significant difference between the natural frequencies of the real and simulation models. To address this issue, the natural frequency error rate κ\kappaκ is introduced as an evaluation index, expressed as follows:

$$\kappa = \left|\frac{f - f_T}{f_T}\right| \times 100\% \tag{5}$$

where f is the natural frequency calculated from the finite element model of the blade, and f_T is the natural frequency measured from the real blade. To apply model updating techniques, the 'zero-setting' procedure for the natural frequency error rate κ is adopted and expressed as follows:

$$\left|(2\pi f_{Ti})^2 \widetilde{\boldsymbol{M}} - E_m^i \frac{\widetilde{\boldsymbol{K}}}{E}\right| = 0 \tag{6}$$

where $\widetilde{\boldsymbol{M}}$ and $\widetilde{\boldsymbol{K}}$ represent the global mass matrix and global stiffness matrix of the blade, respectively; E is the Young's modulus of the real blade; i denotes the modal order of the blade; and E_m^i is the modified Young's modulus corresponding to the natural frequency f_{Ti} measured during the i-order experiment.

2.2. Chebyshev Polynomial Approximation for ULS Curvature

The accuracy of curvature calculation using the central difference method is highly dependent on mesh density. When the mesh is sparse, the central difference method introduces significant computational errors. Conversely, a dense mesh in a two-dimensional structure results in high computational costs. To address these issues, the first kind of Chebyshev polynomial with two variables is utilized to approximate the ULS curvature, enabling effective diagnosis of both the damage location and severity in the blade. First, define the overall deflection vector of the blade under a uniform load as follows:

$$U = \sum_{k=1}^{n}\left\{\frac{\phi_k(i)\sum_{t=1}^{m}\phi_k(t)}{\omega_k^2}\right\} = \boldsymbol{F}\cdot\boldsymbol{L} \tag{7}$$

In the above formula, k represents the modal order of the blade, $\phi_k(i)$ is the displacement of point i on the blade under a unit load at the k-order mode, $\phi_k(t)$ is the displacement of point k on the blade under the unit load, $\boldsymbol{F}$ is the flexibility matrix of the blade after normalization, and $\boldsymbol{L}$ denotes the unit vector of the uniform load surface on the blade structure. The Chebyshev polynomial is then used to approximate the ULS distribution as follows:

$$\phi(x,y) = \sum_{i=1}^{M}\sum_{j=1}^{N} C_{ij} T_i(x)\, T_j(y) \tag{8}$$

Let M and N denote the terms of the Chebyshev polynomials, while $T_i(x)$ and $T_j(y)$ represent the expressions associated with the first-class Chebyshev polynomials. Furthermore, let C_{ij} denote the coefficients of these expressions. To normalize the physical plate domain of the blade, we define two mapping transfer functions:

$$\xi = \frac{2x}{L_x} - 1 \tag{9-a}$$

$$\zeta = \frac{2y}{L_y} - 1 \tag{9-b}$$

In the above expression, L_x and L_y represent the potential regions of damage in the blade, where $\{x,y\} = [0, L_x] \times [0, L_y]$ and $\{\xi,\zeta\} = [-1,1] \times [-1,1]$. Consequently, the Chebyshev polynomial in terms of the variable x can be expressed as:

$$T_1(x) = \frac{1}{\sqrt{\pi}}, \quad T_2(x) = \sqrt{\frac{2}{\pi}}\xi, \tag{10-a}$$

$$T_{i+1}(x) = 2 \times \xi \times T_i(x) - T_{i-1}(x) \tag{10-b}$$

Similarly, the Chebyshev polynomial with respect to the variable y can be expressed as:

$$T_1(y) = \frac{1}{\sqrt{\pi}}, \quad T_2(y) = \sqrt{\frac{2}{\pi}}\zeta, \tag{11-a}$$

$$T_{j+1}(y) = 2 \times \zeta \times T_j(y) - T_{j-1}(y) \tag{11-b}$$

Without loss of generality, Equation (8) can be expressed in matrix form, and the coefficient matrix $\{C_{ij}\}$ can be derived through straightforward fitting procedures :

$$\{C_{ij}\}_{V\times 1} = \left(\left[T(x_i)T(y_j)\right]_{W\times V}^{T}\left[T(x_i)T(y_j)\right]_{W*V}\right)^{-1} \times$$

$$\left[T(x_i)T(y_j)\right]_{W\times V}^{T} \times \{\phi(x_i, y_j)\}_{W\times 1} \tag{12}$$

Because of the orthogonality of the Chebyshev polynomial, respectively, the equation (12) can be approximated as the second and mixed derivatives of x and y :

$$u_{xx}(x,y) = \sum_{i=i}^{M}\sum_{j=1}^{N} c_{ij}\frac{\partial T_i^2(x)}{\partial x^2}T_j(y) \tag{13-a}$$

$$u_{yy}(x,y) = \sum_{i=i}^{M}\sum_{j=1}^{N} c_{ij}T_i(x)\frac{\partial T_j^2(y)}{\partial y^2} \tag{13-b}$$

$$u_{xy}(x,y) = \sum_{i=1}^{M}\sum_{j=1}^{N} c_{ij}\frac{\partial T_i(x)}{\partial x}\frac{\partial T_j(y)}{\partial y} \tag{13-c}$$

Furthermore, a damage index for the blade is developed. As previously noted, damage to the structure results in alterations to both the natural frequency and mode shape. The severity of the damage correlates positively with the extent of change in the vibration mode. By subtracting the ULS curvature of the damaged blade from that of the healthy blade, irregularities in the ULS curvature difference can be detected. Consequently, the damage index can be expressed as follows:

$$d(x_i, y_i) = \left[\alpha_{xx}\left|u_{xx}^D - u_{xx}\right| + \alpha_{yy}\left|u_{yy}^D - u_{yy}\right| + \alpha_{xy}\left|u_{xy}^D - u_{xy}\right|\right]^2 \tag{14}$$

In the formula above, u_{xx}, u_{yy} and u_{xy} represent the axial, radial, and mixed curvature of the healthy blade, respectively. Conversely, u_{xx}^D, u_{yy}^D and u_{xy}^D denote the axial, radial, and mixed curvature of the damaged blade. Additionally, α_{xx}, α_{yy} and α_{xy} are weight factors, with values ranging from 0 to 1 in each of the three directions.

The weight factor in equation (14) can be regarded as reflecting the importance of second-order derivative differences in the corresponding direction, used to adjust the contribution of curvature changes in that direction to the damage indicator. The weight factor is determined by factors such as the material, geometry, and damage type of the structure. For an ideal scenario involving an isotropic square plate with a through-hole, the weight coefficient can be set to $\alpha_{xx}=\alpha_{yy}=\alpha_{xy}=1$. The optimal distribution value of the weight coefficient for the corresponding case can be determined through experiments combined with optimization algorithms.

3. Experimental verification

3.1. Experiment description

In this section, a dynamic analysis of the blade model is conducted, and the enhanced ULS curvature-based damage detection method is employed to identify both the location and severity of the damage. A schematic representation of the entire experimental arrangement is provided in Figure 2. The experimental setup for measuring the first five natural frequencies of the blade model using a laser vibrometer is illustrated in Figure 3. The terminal of the data acquisition system, depicted in Figure 3-a, consists of a signal generator (PSV-F-500), a host computer (PSV-W-500), and a power amplifier (2100E31-400). The front end of the system, shown in Figure 3-b, includes the fully digital scanning laser vibrometer (PSV-I-500), the shaker (2060E), and the sample blade.

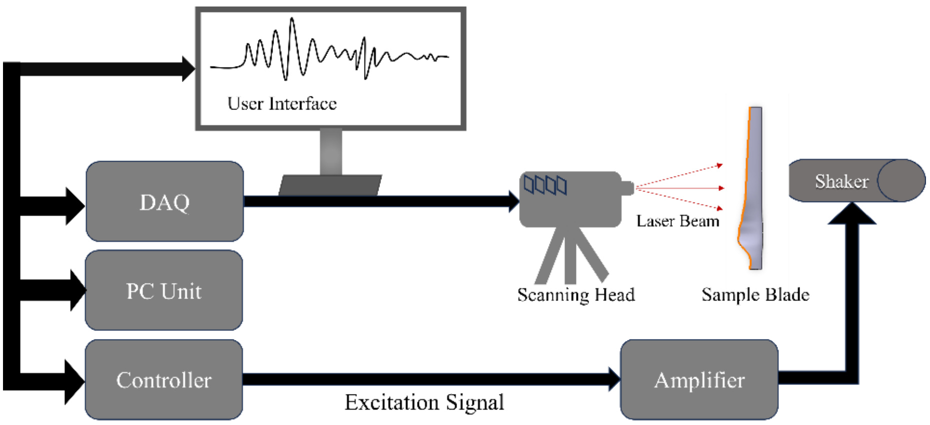

Figure 2. Experimental device connection diagram.

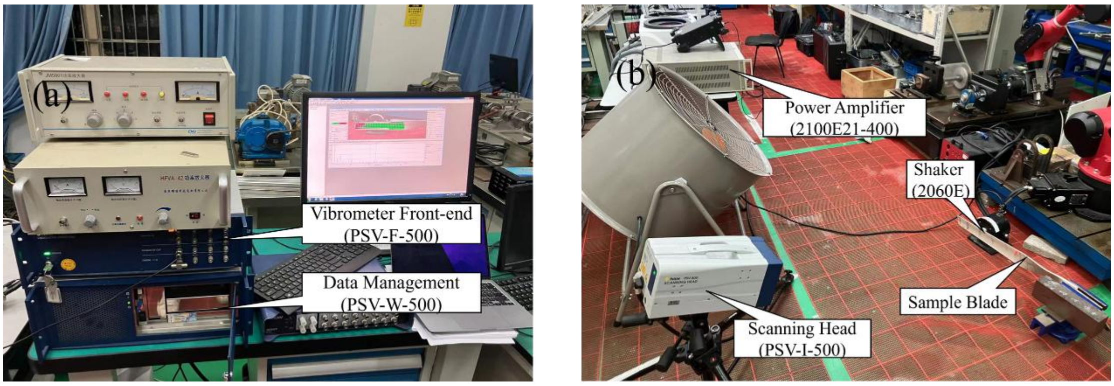

Figure 3. The experimental setup of WT blade.

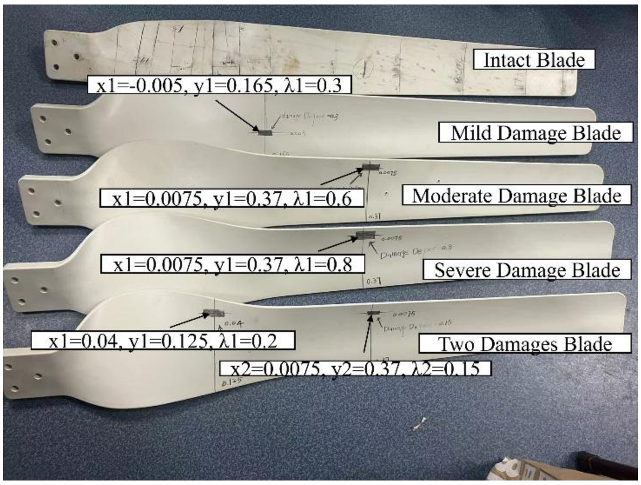

Figure 4. The damage type of WT blade.

The material of the blade is regarded as fiberglass, and its material properties are assumed to be isotropic. One end of the blade is fully clamped, while the other end is free. The free end of the blade is subjected to vibration induced by the vibration exciter. A laser beam emitted by the laser head is directed onto the surface of the blade, and the reflected laser beam is received. Interference effects are applied to detect the minute displacement changes on the blade surface, with variations in displacement corresponding to different damage conditions.

The extent of damage is quantified by the crack depth, and the corresponding formula is provided as follows:

$$\lambda_i = \frac{h_i}{H} \tag{15}$$

Here, λ_i represents the damage degree of the i-th crack, h_i denotes the depth of the i-th crack, and H is the thickness of the blade at the damaged location. The damage severity is further classified as follows: when $0 < \lambda \leq 0.3$, the damage is considered mild; when $0.3 < \lambda \leq 0.6$, the damage is classified as moderate; and severe damage is identified when $\lambda > 0.6$. Accordingly, four distinct damage levels are defined, with detailed damage information provided in Table 1 and Figure 4. The damage discussed below refers to open cracks.

Table 1. Damage information for four types of damaged blades

Case	Damage information					
	x_1	y_1	λ_1	x_2	y_2	λ_2
Blade with mild damage	-0.005	0.165	0.3			
Blade with moderate damage	0.0075	0.37	0.6			
Blade with severe damage	0.0075	0.37	0.8			
Blade with two damages	0.04	0.125	0.2	0.0075	0.37	0.15

The laser vibrometer leverages the coherence and wave properties of laser light to detect optical path variations caused by the motion of an object. When the WT blade vibrates, the reflected measurement beam undergoes a Doppler shift due to the transverse reciprocating motion of its surface. This shift is utilized to calculate the vibration velocity of the blade. Finally, high-precision vibration parameters are obtained by the FFT analysis.

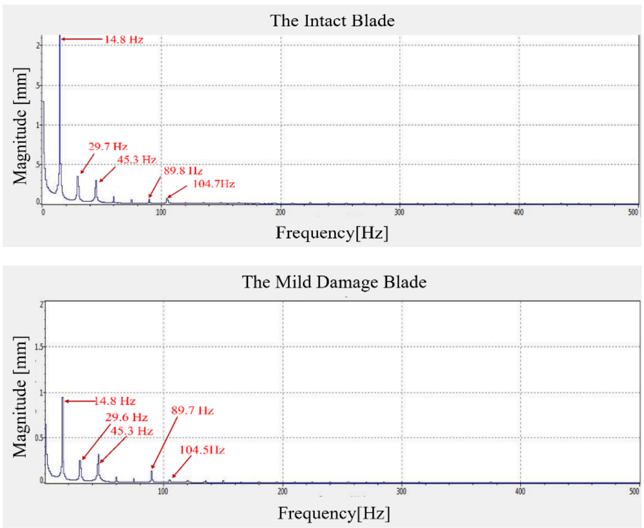

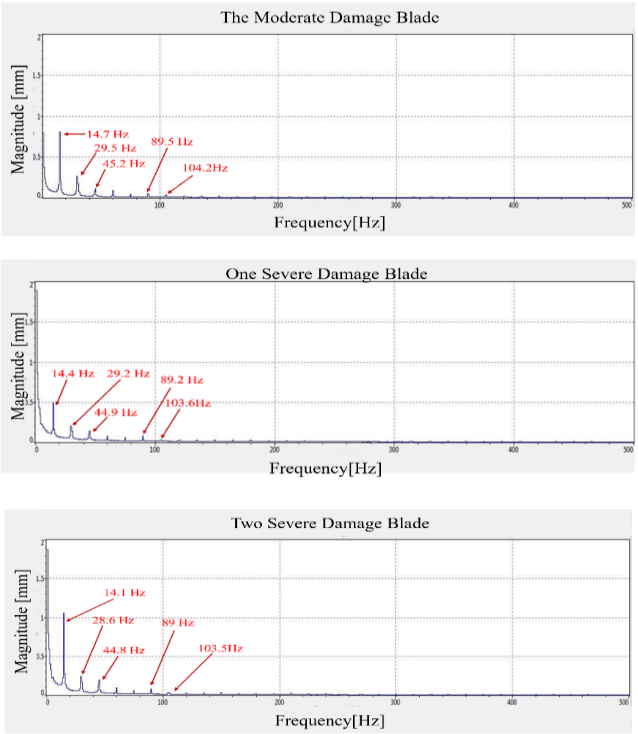

Figure 5. Spectrum diagram of the five blade models under harmonic excitation signals.

The key parameters of the experiment were selected as follows: a sampling frequency bandwidth of 1.25 kHz, a sampling frequency of 5 kHz, and a sampling duration of 1.5 s. The spectral diagram of the final scanning acquisition is presented in Figure 5. The measured natural frequencies of the intact blade are provided in Table 2 for the calibration of the blade simulation model. From Table 2, the first order frequency is one-third of the third order frequency and the fourth order frequency is twice as much as the third frequency approximately. According to the reference[30], the experimentally measured data is within in a reasonable range.

Table 2. Experimentally measured natural frequency of healthy blade specimen.

Case	f_1(Hz)	f_3(Hz)	f_4(Hz)	f_5(Hz)
Intact blade	14.8	45.3	89.8	104.7

Using small sample trials instead of large amounts of experimental data significantly achieves cost reduction and efficiency improvement [32,34]. The feasibility of the method is validated by combining small-scale blade experiments with simulations. The data obtained from modal analysis show an error within 1.5% compared to experimental data. The method is further applied to the NREL 5MW wind turbine blade model to verify its practicality. By combining FEA with small sample test data, the cost and time required for large amounts of experimental data are significantly reduced.

3.2. Modal analysis

Based on the measurements of the dimensions and contour of the selected 0.7 m intact physical blade model, as shown in Figure 6, modeling software was utilized to construct a scaled model of the actual blade, as illustrated in Figure 7. Additionally, a model updating method was employed to ensure that the three-dimensional model closely aligns with the physical blade. The updated Young's modulus values are provided in Table 3.

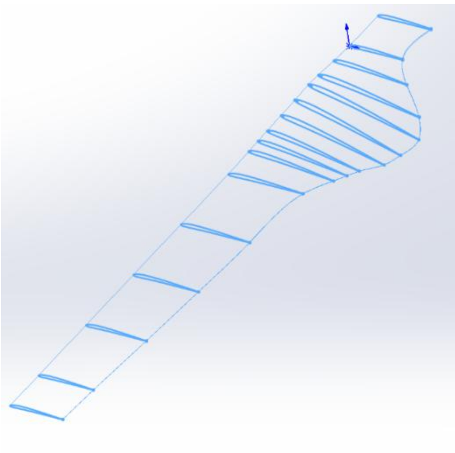

Figure 6. The quarter chord of the WT blade model profiles.

Figure 7. 3D solid model of the intact blade.

Table 3. The modified Young’s modulus.

Mode Number	1	3	4	5
E_m^i(Pa)	2.6e10	6.5e9	4.4e9	4.4e9

Modal analysis of the modified blade model was conducted by using COMSOL. The natural frequencies and mode shapes of the healthy blade model are presented in Table 4 and Figure

8. In Table 5, the natural frequency error rate κ is maintained within 1%. Note that the second-order simulation results for the blade were excluded due to experimental equipment limitations; only the transverse vibration of the blade was measured, and the second-order torsional natural frequency obtained from the simulation could not be directly compared with the second-order natural frequency measured experimentally.

Table 4. The natural frequencies obtained by FEM.

Case	f_1(Hz)	f_3(Hz)	f_4(Hz)	f_5(Hz)
Intact blade	14.724	45.515	89.287	104.59

Table 5. The error rate of the natural frequencies between FEM and experiment.

Model type	f_1(Hz)	f_3(Hz)	f_4(Hz)	f_5(Hz)
Experimental frequency(Hz)	14.8	45.3	89.8	104.7
FEM frequency(Hz)	14.724	45.515	89.287	104.59
κ(%)	0.51	0.47	0.57	0.1

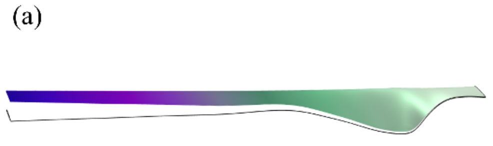

(a) The first order mode shape

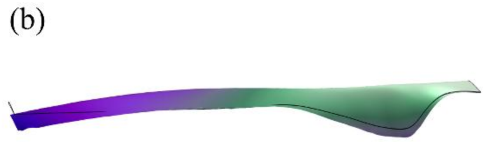

(b) The second order mode shape

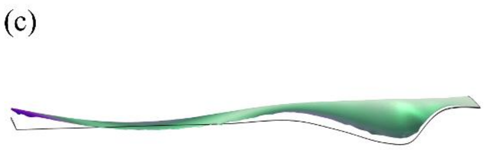

(c) The third order mode shape

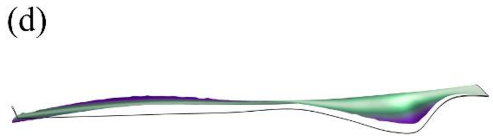

(d) The fifth order mode shape

Figure 8. WT blade's model shape.

Table 6. Four natural frequencies of different damaged WT blades with the experiment.

Case	f_1(Hz)	f_3(Hz)	f_4(Hz)	f_5(Hz)
Blade with mild damage	14.8	45.3	89.7	104.5
Blade with moderate damage	14.7	45.2	89.5	104.2
Blade with severe damage	14.4	44.9	89.2	103.6
Blade with two damage	14.1	44.8	89	103.5

Through the previous steps, the blade model and the actual blade have been standardized with greater precision, enabling the introduction of damage to the blade model. In the simulation, the local elastic modulus of the blade is reduced to simulate damage, effectively avoiding errors associated with grid changes due to notched damage. Tables 6 and 7 present the natural frequency values obtained from the experiment and the FEM simulation with four types of damaged blade specimens, respectively.

Table 7. Four natural frequencies of different damaged WT blades with the FEM.

Case	f_1(Hz)	f_3(Hz)	f_4(Hz)	f_5(Hz)
Blade with mild damage	14.719	45.5	89.274	104.32
Blade with moderate damage	14.52	45.33	89.085	104
Blade with severe damage	14.16	44.918	88.652	103.34
Blade with two damage	13.99	44.804	88.521	102.73

3.3. Damage Assessment

In the previous section, the fourth-order natural frequencies of the blade obtained from both experiments and simulations were presented. It is evident from the tables that the natural frequencies of the blade decrease as the severity of damage increases, with the impact of varying degrees of damage on the lower-order natural frequencies being less pronounced than that on the higher-order natural frequencies. In summary, while changes in natural frequency can indicate the presence of damage and provide an approximate assessment of its severity, it is essential to analyze the mode shape vector to accurately determine the specifics of the damage.

To reduce computational complexity, the ULS curvature at the nodes in this section was calculated to identify the specific location and severity of damage by pinpointing intervals with significant differences in the mode shape vector between the healthy and damaged blades. Consequently, Chebyshev-ULS curves for four groups of damaged blade models were computed, with $M = N = 5$ for the Chebyshev polynomial to achieve a smooth fitting effect, as illustrated in Figure 9. When damage occurs at a site with a greater curvature, the influence of the damage is more significant. Even when the damage degree = 0.3, the affected area is no smaller than that when the damage degree = 0.6. From both the forward and top views, the damage severity and location of the actual blade were found to be completely consistent.

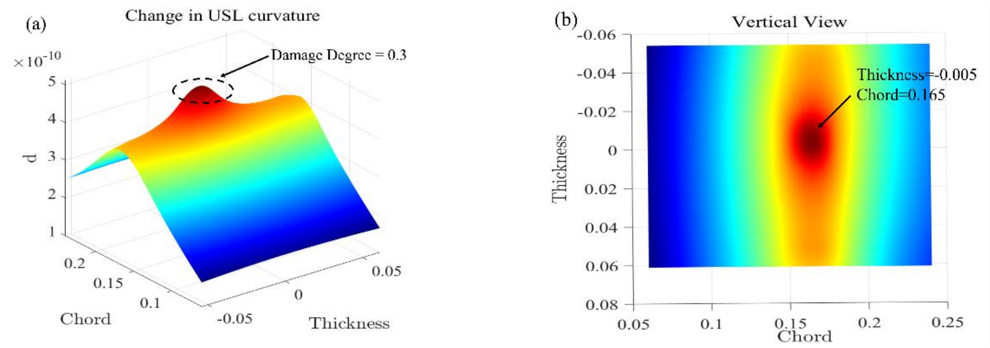

Figure 9. The damage information diagrams of Case 1 using the first order frequency.

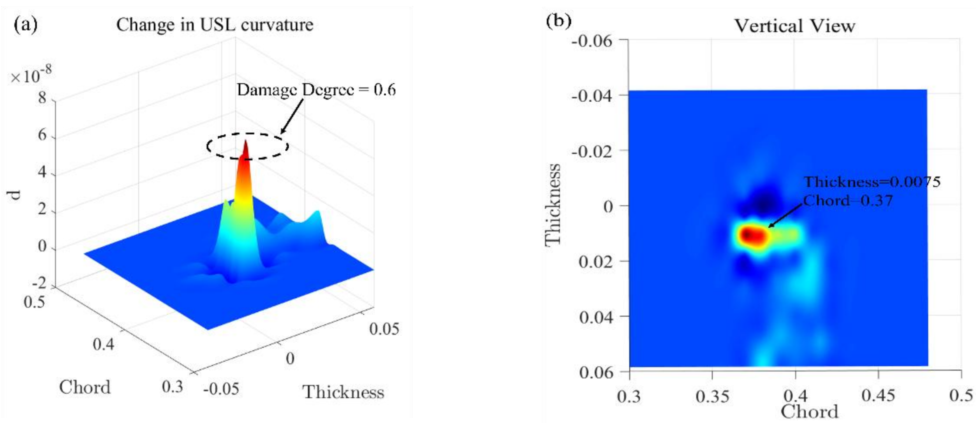

Figure 10. The damage information diagrams of Case 2 using the first order frequency.

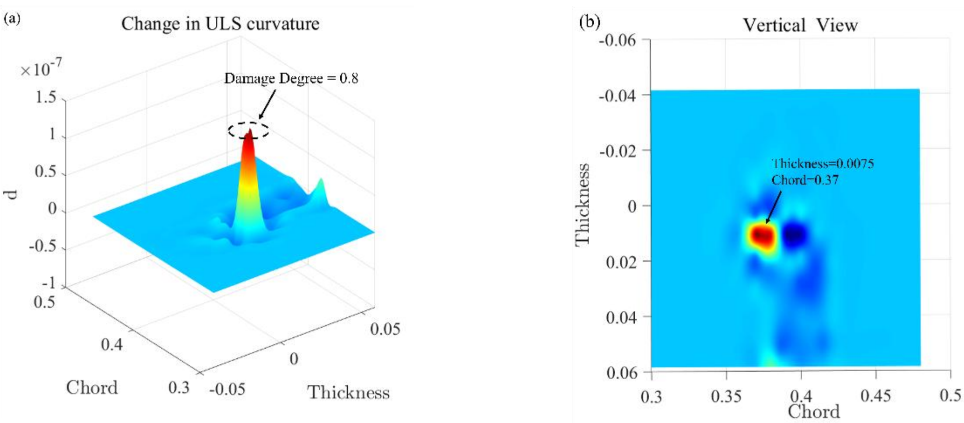

Figure 11. The damage information diagrams of Case 3 using the first order frequency.

Figures 10 and 11 depict Case 2 (moderate damage) and Case 3 (severe damage), respectively. In the experiment, these two cases serve as the control group. The control variable method was employed to assess the sensitivity of the approach to the degree of damage. A comparison of Figures 10-a and 11-a reveals that the peak value for Case 3 is significantly higher than that for Case 2. In Case 4 (double-damaged blades), the Young's modulus of the damaged areas was reduced by 20% and 15%, respectively, to simulate mild transverse damage as observed in the experiment. The weight factors used in the first two cases, where the two wave peaks were nearly equal to 1, did not effectively differentiate the severity of the damage. Consequently, α_{yy} in Equation (14) was set to 0.6. The resulting data is presented in Figure 12-a.

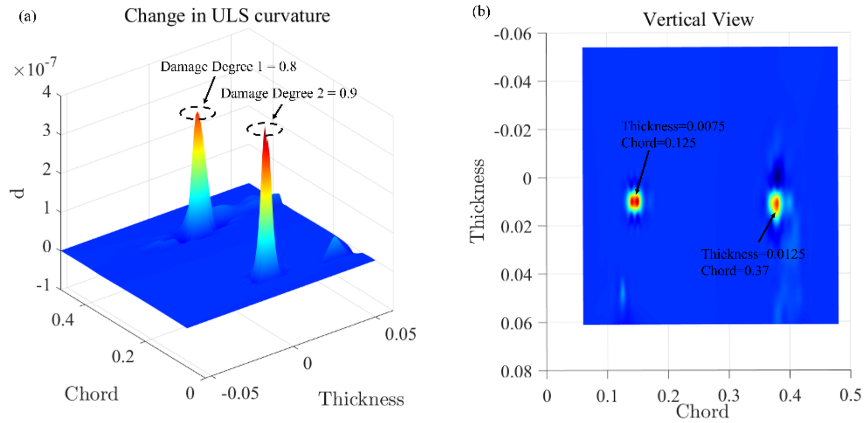

Figure 12. The damage information diagrams of Case 4 using the first order frequency.

4. Numerical example

4.1. NREL 5MW wind turbine blade model

The NREL 5MW wind turbine blade is widely used in various experimental testing and analysis. In order to validate the effectiveness of this method, a three-dimensional model of the NREL 5MW WT blade was constructed in COMSOL and 280 Chebyshev-ULS measuring nodes were selected totally. It consists of 19 distinct airfoil sections from the tip to the root, with a geometric length of 61.5m. From the viewpoints of aerodynamics and blade structural design, NACA 64-618 and DU 99-W-405 were respectively applied to the tip area and root of the blade. Smooth transitions between these two extreme sections were achieved through other airfoils of the DU series, as depicted in Figure 13. In general, the blade model is an aerodynamic shell with rubber segments along the trailing edge. As shown in Figure 14, the whole NREL 5MW WT blade model is generated through a sweeping mesh operation, resulting in 5,984 boundary elements and 1,652 edge elements.

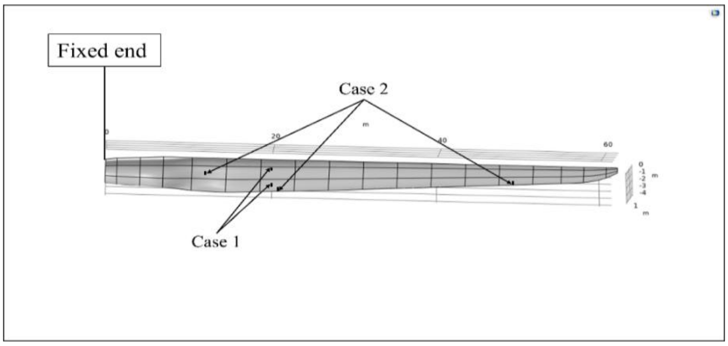

Figure 13. NREL 5MW WT blade 3D solid model.

Two sets of damage cases were respectively established. Among them, in order to verify the anti-interference performance of the detection method against the environment, a 4% sinusoidal noise was applied in the second set of cases. The following formula was adopted to simulate the sinusoidal noise:

$$NS_{Noise} = (4\% \times \sin(10\pi t) + 1) \times NS \tag{16}$$

where NS represents the node displacement data obtained from modal analysis, and NS_{Noise} denotes the node displacement data after noise has been applied. The damage parameters of the two cases are:

Case 1. $x_1 = 20.05\ m$, $y_1 = 0.75\ m$, $\lambda_1 = 0.8$; $x_2 = 20.05\ m$, $y_2 = 1\ m$, $\lambda_2 = 0.6$, as shown in Figure 12.

Case 2. $x_1 = 10.2\ m$, $y_1 = 0\ m$, $\lambda_1 = 0.5$; $x_2 = 20\ m$, $y_2 = -2\ m$, $\lambda_2 = 0.3$; $x_3 = 50.5\ m$, $y_3 = -1.7\ m$, $\lambda_3 = 0.5$, as shown in Figure 12.

Figure 14. Grid subdivision of NREL 5MW WT blade.

4.2. Results discussions

The first natural frequency and modal shape of the NREL 5MW wind turbine were obtained through finite element analysis, and noise was introduced in Example 2. The surface diagram was generated using Chebyshev-ULS fitting, as illustrated in Figure 16 and Figure 17.

Through the damage assessment of the NREL 5MW large wind turbine blades and the analysis of the results from Example 1, it was determined that the accuracy of damage localization remains intact. However, in evaluating damage severity, when the evaluation factor matches that of the test blade, $\alpha_{xx} = \alpha_{yy} = \alpha_{xy} = 0.4$, the damage assessment results are not pronounced. Therefore, the damage area can be expanded by doubling the values of α_{xx} and α_{xy}, as illustrated in Figure 15.

The results of Example 2 were analyzed, with evaluation factors set to $\alpha_{xx} = \alpha_{xy} = 0.8$ and $\alpha_{yy} = 0.4$. While noise did not affect the damage evaluation, it had a minor impact on damage localization, with the location error remaining below 0.2%.

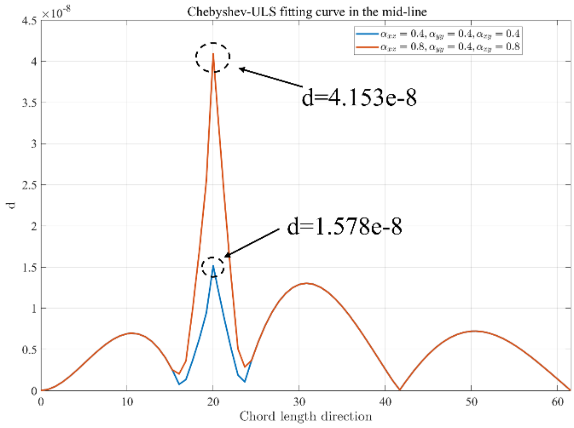

Figure 15. Chebyshev-ULS fitting curve in NREL 5MW WT blade mid-line.

It is important to note that the adjustment of the evaluation factors has a minimal impact on the undamaged area, with the calculated average difference exceeding four orders of magnitude. As shown in Figure 15, this is one of the notable advantages of Chebyshev-ULS. Furthermore, the adjustment of damage factors serves to enlarge or reduce the overall assessment without affecting the evaluation results.

Compared to the second order central differencing curvature method, noise frequently induces abrupt variations at specific points on the blade, which can impact the accuracy of damage localization and even mislead the estimation of damage quantity. The proposed method effectively addresses this limitation by mitigating the influence of single-point noise. Furthermore, even in cases where noise within a particular region is exceptionally intense, the distortion caused by irregular noise can be minimized through the application of Chebyshev polynomial fitting.

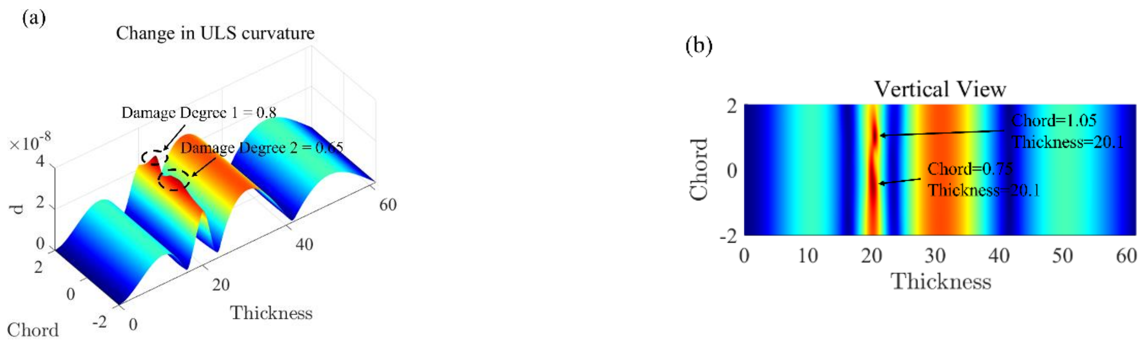

Figure 16. The damage information diagrams of Case 1 using the first order frequency.

Figure 17. The damage information diagrams of Case 2 using the first order frequency.

4.3. Comparison of Chebyshev-ULS method and SVD-WOA method

Compared to the SVD-WOA method[32], it combined optimization algorithm is employed to locate and assess damage. However, it suffers from two shortcomings: First, when the damage locations are in close proximity, the adjacent damage regions can interact, resulting in a stack effect that forms wave peaks, as illustrated in Figure 18. This effect is influenced by both the distance and severity of the damage, as singular value decomposition (SVD) does not effectively mitigate the regional impact of the damage. Secondly, the accuracy of damage evaluation is highly dependent on the completeness of the optimization dataset. Secondly, when multiple damages are present, the assessment becomes unstable, as shown in Figure 19. If the degrees of damage are exactly equal, the database, which is constructed solely based on natural frequencies, may result in structural ambiguity. In this case, multiple damage combinations can correspond to the same natural frequency.

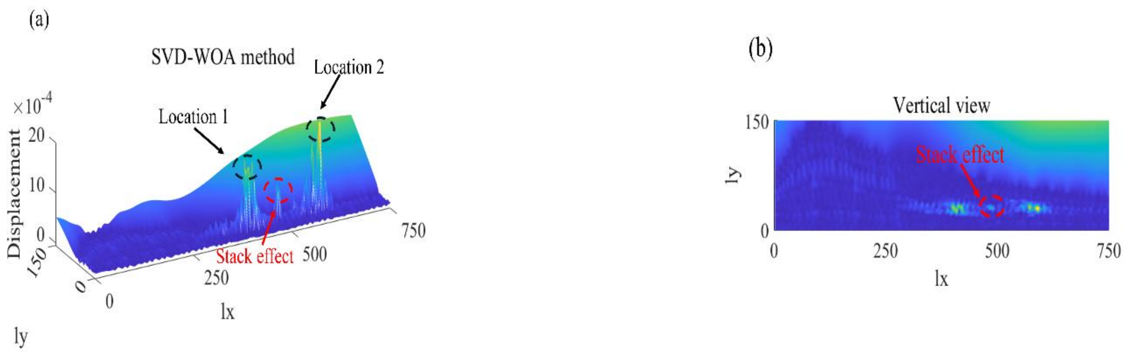

Figure 18. The diagrams of two damage WT blade using SVD-WOA method.

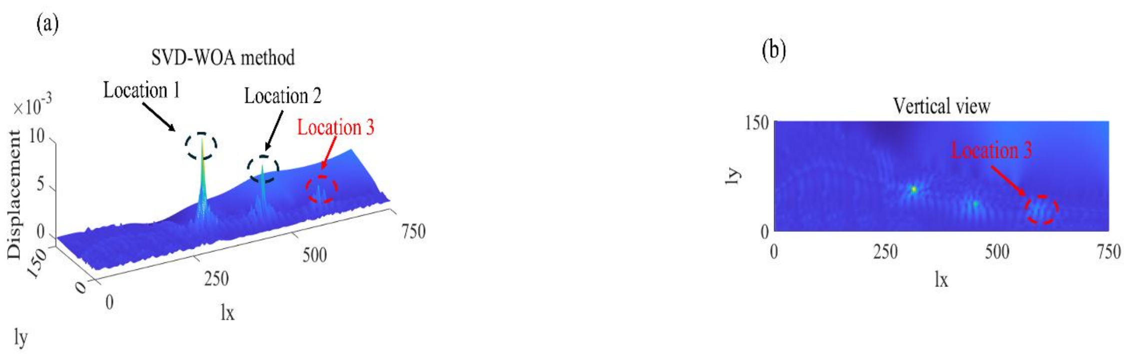

Figure 19. The diagrams of three damage WT blade using SVD-WOA method.

5. Conclusion

This paper presents a novel method for locating and evaluating structural damage in blades, utilizing Chebyshev polynomial approximation to compute ULS curvature. By replacing the central difference calculation with Chebyshev polynomials, the method reduces the number of required measuring points while maintaining accuracy. The flexibility matrix demonstrates increased sensitivity to damage and enhanced robustness, allowing the first natural frequency and mode of the blade to effectively indicate the severity and location of damage. Numerical simulations and experiments were conducted to validate the method's operability and accuracy. Finally, Chebyshev-ULS was applied to the NREL 5MW wind turbine blade model. For large blades, sensitivity tends to decrease; however, by adjusting the scale function factors to amplify the impact of damage, the method still achieves high accuracy. In addition, this method still has certain limitations for detecting damage in wind turbine blades, as it is not sufficiently sensitive to internal dents and small deformations of the blade. On balance, the approach for diagnosing structural faults in wind power blades using modal parameters is further optimized, providing a new direction for future research.

Acknowledgments

The authors are grateful to the support of National Natural Science Foundation of China (No. 52005373 and 12202318), the Zhejiang Provincial Natural Science Foundation of China (LQ21E050002) ,Wenzhou Municipal Science and Technology Bureau, China (No. G2020014), and Innovation Project of Guangxi Graduate Education(YCBZ2023135).

Reference

1. Tehrani K, Beikbabaei M, Mehrizi-Sani A, Jamshidi M. A smart multiphysics approach for wind turbines design in industry 5.0. Journal of Industrial Information Integration. 2024;42(0022460X). https://doi:10.1016/j.jii.2024.100704.
2. Shakya P, Thomas M, Seibi AC, Shekaramiz M, Masoum MS. Fluid-structure interaction and life prediction of small-scale damaged horizontal axis wind turbine blades. Results in Engineering. 2024;23. https://doi:10.1016/j.rineng.2024.102388.
3. Fang H, Feng Y, Wei X, Xiong J. Wind turbine blade damage aerodynamic profile analysis and its repair techniques. Energy Reports. 2023;9:1-10. https://doi:10.1016/j.egyr.2023.04.041.
4. Kang S, He Y, Li W, Liu S. Research on Defect Detection of Wind Turbine Blades Based on Morphology and Improved Otsu Algorithm Using Infrared Images. Computers, Materials & Continua. 2024;81(1):933-49. https://doi:10.32604/cmc.2024.056614.
5. Oliveira MA, Simas Filho EF, Albuquerque MCS, Santos YTB, da Silva IC, Farias CTT. Ultrasound-based identification of damage in wind turbine blades using novelty detection. Ultrasonics. 2020;108. https://doi:10.1016/j.ultras.2020.106166.
6. Rizk P, Rizk F, Karganroudi SS, Ilinca A, Younes R, Khoder J. Advanced wind turbine blade inspection with hyperspectral imaging and 3D convolutional neural networks for damage detection. Energy and AI. 2024;16. https://doi:10.1016/j.egyai.2024.100366.
7. Wang B, Sun W, Wang H, Xu T, Zou Y. Research on rapid calculation method of wind turbine blade strain for digital twin. Renewable Energy. 2024;221. https://doi:10.1016/j.renene.2023.119783.
8. Chen Y, Griffith DT. Experimental and numerical full-field displacement and strain characterization of wind turbine blade using a 3D Scanning Laser Doppler Vibrometer. Optics & Laser Technology. 2023;158. https://doi:10.1016/j.optlastec.2022.108869.
9. Khazaee M, Derian P, Mouraud A. A comprehensive study on Structural Health Monitoring (SHM) of wind turbine blades by instrumenting tower using machine learning methods. Renewable Energy. 2022;199:1568-79. https://doi:10.1016/j.renene.2022.09.032.
10. Song F, Han Y, William Heath A, Hou M. Structural damage detection of floating offshore wind turbine blades based on Conv1d-GRU-MHA network. Engineering Failure Analysis. 2024;166. https://doi:10.1016/j.engfailanal.2024.108896.
11. Xu D, Liu PF, Chen ZP, Leng JX, Jiao L. Achieving robust damage mode identification of adhesive composite joints for wind turbine blade using acoustic emission and machine learning. Composite Structures. 2020;236. https://doi:10.1016/j.compstruct.2019.111840.
12. Ren C, Xing Y. An efficient active learning Kriging approach for expected fatigue damage assessment applied to wind turbine structures. Ocean Engineering. 2024;305. https://doi:10.1016/j.oceaneng.2024.118034.
13. Zhang L, Wang X, Lu S, Jiang X, Ma C, Lin L, et al. Fatigue damage monitoring of repaired composite wind turbine blades using high-stability buckypaper sensors. Composites Science and Technology. 2022;227. https://doi:10.1016/j.compscitech.2022.109592.

14. Li J, Dao MH, Le QT. Data-driven modal parameterization for robust aerodynamic shape optimization of wind turbine blades. Renewable Energy. 2024;224. https://doi:10.1016/j.renene.2024.120115.
15. Pacheco-Chérrez J, Cárdenas D, Delgado-Gutiérrez A, Probst O. Operational modal analysis for damage detection in a rotating wind turbine blade in the presence of measurement noise. Composite Structures. 2023;321. https://doi:10.1016/j.compstruct.2023.117298.
16. Song M, Partovi Mehr N, Moaveni B, Hines E, Ebrahimian H, Bajric A. One year monitoring of an offshore wind turbine: Variability of modal parameters to ambient and operational conditions. Engineering Structures. 2023;297. https://doi:10.1016/j.engstruct.2023.117022.
17. Chen Y, Griffith DT. Blade mass imbalance identification and estimation for three-bladed wind turbine rotor based on modal analysis. Mechanical Systems and Signal Processing. 2023;197. https://doi:10.1016/j.ymssp.2023.110341.
18. Dolinski L, Krawczuk M. Analysis of Modal Parameters Using a Statistical Approach for Condition Monitoring of the Wind Turbine Blade. Applied Sciences. 2020;10(17). https://doi:10.3390/app10175878.
19. Selna LG, Shilling-Burg HT, JR., Kerr PA. Finite Element Analysis of Dental Structures - Axisymmetric and Plane Stress Idealizations. Journal of Biomedical Materials Research. 1975;9:237-52.
20. Pai PF, G.Young L. Damage detection of beam using operational deflection shapes. International Journal of Soilds and Structures. 2001;38:3161-92.
21. Viola E, Federici L, Nobile L. Detection of crack location using cracked beam element for structural analysis. Theoretical and Applied Fracture Mechanics. 2001;36:23-5.
22. Rodríguez R, Escobar JA, Gómez R. Damage detection in instrumented structures without baseline modal parameters. Engineering Structures. 2010;32(6):1715-22. https://doi:10.1016/j.engstruct.2010.02.021.
23. Wei F, Pizhong Q. Vibration-based Damage Identification Methods: A Review and Comparative Study. Structural Health Monitoring. 2010;10(1):83-111. https://doi:10.1177/1475921710365419.
24. Huang M, Li X, Lei Y, Gu J. Structural damage identification based on modal frequency strain energy assurance criterion and flexibility using enhanced Moth-Flame optimization. Structures. 2020;28:1119-36. https://doi:10.1016/j.istruc.2020.08.085.
25. Wang N, Zhu R-h, Wang Q-m, Zheng J-h, Zhang J-b. A method for quantitative damage identification in a high-piled wharf based on modal strain energy residual variability. Ocean Engineering. 2022;254. https://doi:10.1016/j.oceaneng.2022.111314.
26. Gao J-X, An Z-W, Ma Q, Bai X-Z. Residual strength assessment of wind turbine rotor blade composites under combined effects of natural aging and fatigue loads. Eksploatacja i Niezawodność – Maintenance and Reliability. 2020;22(4):601-9. https://doi:10.17531/ein.2020.4.3.
27. Kim D-G, Lee S-B. Structural damage identification of a cantilever beam using excitation force level control. Mechanical Systems and Signal Processing. 2010;24(6):1814-30. https://doi:10.1016/j.ymssp.2010.02.007.
28. Sung SH, Jung HJ, Jung HY. Damage detection for beam-like structures using the normalized curvature of a uniform load surface. Journal of Sound and Vibration. 2013;332(6):1501-19. https://doi:10.1016/j.jsv.2012.11.016.
29. Wu D, Law SS. Damage localization in plate structures from uniform load surface curvature. Journal of Sound and Vibration. 2004;276(1-2):227-44. https://doi:10.1016/j.jsv.2003.07.040.
30. Jiang Y, Sun J, Lin Q, Xiang J. A two-stage method to detect damages in aluminum plates using curvature modal shape subtraction indicator and particle swarm optimization. Thin-Walled Structures. 2023;185. https://doi:10.1016/j.tws.2023.110560.
31. Bai R, Wang H, Sun W, Shi Y. Fault diagnosis method for rotating machinery based on SEDenseNet and Gramian Angular Field. Eksploatacja i Niezawodność – Maintenance and Reliability. 2024;26(4). https://doi:10.17531/ein/191445.
32. Wang Y, Liang M, Xiang J. Damage detection method for wind turbine blades based on dynamics analysis and mode shape difference curvature information. Mechanical Systems and Signal Processing. 2014;48(1-2):351-67. https://doi:10.1016/j.ymssp.2014.03.006.
33. Cadoret A, Denimal-Goy E, Leroy J-M, Pfister J-L, Mevel L. Damage detection and localization method for wind turbine rotor based on Operational Modal Analysis and anisotropy tracking. Mechanical Systems and Signal Processing. 2025;224. https://doi:10.1016/j.ymssp.2024.111982.
34. Jiang H, Jiang Y, Xiang J. Method using singular value decomposition and whale optimization algorithm to quantitatively detect multiple damages in turbine blades. Structural Health Monitoring. 2023;23(2):1025-36. https://doi:10.1177/14759217231173589.
35. Pacheco-Chérrez J, Probst O. Vibration-based damage detection in a wind turbine blade through operational modal analysis under wind excitation. Materials Today: Proceedings. 2022;56:291-7. https://doi:10.1016/j.matpr.2022.01.159.

36. Yang C, Li P, Lang X, Wu J. A novel NMF-DiCCA deep learning method and its application in wind turbine blade icing failure identification. Eksploatacja i Niezawodność – Maintenance and Reliability. 2024;26(4). https://doi:10.17531/ein/190381.